

Accepted Article

Title: Discovery of a series of 2-((1-phenyl-1H-imidazol-5-yl)methyl)-1H-indoles as indoleamine 2,3-dioxygenase 1 (IDO1) inhibitors

Authors: Donald F Weaver, Yong Zheng, Paul M. Stafford, Kurt R. Stover, Darapaneni Chandra Mohan, Mayuri Gupta, Eric C. Keske, Paolo Schiavini, Laura Villar, Fan Wu, Alexander Kreft, Kiersten Thomas, Elana Raaphorst, Jagadeesh P. Pasangulapati, Siva R. Alla, Simmi Sharma, Ramana R. Mittapalli, Irina Sagamanova, Mark A. Reed, and Shea L. Johnson

This manuscript has been accepted after peer review and appears as an Accepted Article online prior to editing, proofing, and formal publication of the final Version of Record (VoR). This work is currently citable by using the Digital Object Identifier (DOI) given below. The VoR will be published online in Early View as soon as possible and may be different to this Accepted Article as a result of editing. Readers should obtain the VoR from the journal website shown below when it is published to ensure accuracy of information. The authors are responsible for the content of this Accepted Article.

To be cited as: *ChemMedChem* 10.1002/cmdc.202100107

Link to VoR: <https://doi.org/10.1002/cmdc.202100107>

COMMUNICATION

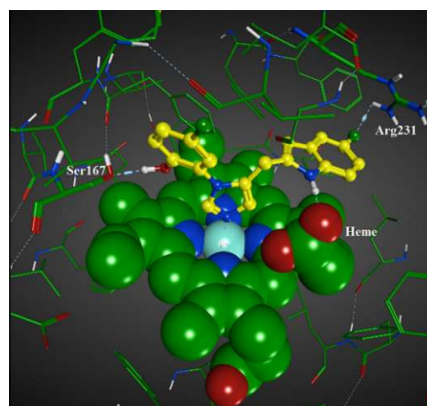
Discovery of a series of 2-((1-phenyl-1H-imidazol-5-yl)methyl)-1H-indoles as indoleamine 2,3-dioxygenase 1 (IDO1) inhibitors

Yong Zheng,^[a] Paul M. Stafford,^[a] Kurt R. Stover,^[a] Darapaneni Chandra Mohan,^[a] Mayuri Gupta,^[a] Eric C. Keske,^[a] Paolo Schiavini,^[a] Laura Villar,^[a] Fan Wu,^[a] Alexander Kreft,^[a] Kiersten Thomas,^[a] Elana Raaphorst,^[a] Jagadeesh P. Pasangulapati,^[a] Siva R. Alla,^[a] Simmi Sharma,^[a] Ramana R. Mittapalli,^[a] Irina Sagamanova,^[a] Shea L. Johnson,^[a] Mark A. Reed,^{[a],[b]} Donald F. Weaver*^{[a],[b],[c]}

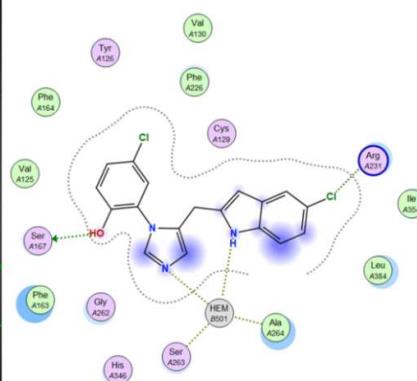
Dedicated to the memory of Prof. Walter A. Szarek

- [a] Dr. Y. Zheng, P. M. Stafford, Dr. K. R. Stover, Dr. D. C. Mohan, Dr. M. Gupta, Dr. E. C. Keske, Dr. P. Schiavini, Dr. L. Villar, Dr. F. Wu, Dr. A. Kreft, K. Thomas, E. Raaphorst, J. P. Pasangulapati, Dr. S. R. Alla, Dr. S. Sharma, Dr. R. R. Mittapalli, Dr. I. Sagamanova, Dr. S. L. Johnson, Prof. M. A. Reed, Prof. D. F. Weaver
Krembil Research Institute
University Health Network
60 Leonard Avenue, Toronto, ON M5T 2S8, Canada
Corresponding author's E-mail: donald.weaver@uhnresearch.ca
- [b] Prof. M. A. Reed, Prof. D. F. Weaver
Department of Chemistry
University of Toronto, Toronto, ON M5S 3H6, Canada
- [c] Prof. D. F. Weaver
Department of Medicine, Division of Neurology
University of Toronto, Toronto, ON M5S 1A8, Canada

Supporting information for this article is given via a link at the end of the document.



Abstract: Indoleamine 2,3-dioxygenase 1 (IDO1) is a promising therapeutic target in cancer immunotherapy and neurological disease. Thus, searching for highly active inhibitors for use in human cancers is now a focus of widespread research and development efforts. In this study, we report the structure-based design of 2-(5-imidazolyl)indole derivatives, a series of novel IDO1 inhibitors which have been designed and synthesized based on our previous study using *N*1-substituted 5-indoleimidazoles. Among these, we have identified one with a strong IDO1 inhibitory activity ($IC_{50} = 0.16 \mu\text{M}$, $EC_{50} = 0.3 \mu\text{M}$). Structural-activity relationship (SAR) and computational docking simulations suggest that a hydroxyl group favorably interacts with a proximal Ser167 residue in Pocket A, improving IDO1 inhibitory potency. The brain penetrance of potent compounds was estimated by calculation of the Blood Brain Barrier (BBB) Score and Brain Exposure Efficiency (BEE) Score. Many compounds had favorable scores and the two most promising compounds were advanced to a pharmacokinetic study which demonstrated that both compounds were brain penetrant. We have thus discovered a flexible scaffold for brain penetrant IDO1 inhibitors, exemplified by several potent, brain penetrant, agents. With this promising scaffold, we provide herein a basis for further development of brain penetrant IDO1 inhibitors.



Introduction

Over the last two decades, immunotherapy has arisen as a powerful approach to the treatment of cancers.^[1,2] IDO1 is a heme-containing monomeric enzyme which catalyzes the catabolism of tryptophan in the first rate-limiting step to *N*-formylkynurenine via the oxidative cleavage of the C2–C3 indole double bond.^[3] *N*-formylkynurenine is further converted to kynurenine and a series of biologically active metabolites, including the final product nicotinamide adenine dinucleotide (NAD).^[4] IDO1 regulates the immune response by producing biologically active kynurenine pathway metabolites.^[5] In the tumor microenvironment, IDO1 is found as a key mediator of innate and adaptive immunity.^[5]

IDO1 is highly expressed by tumor cells to escape a potentially effective immune response via depletion of *L*-tryptophan in the tumor microenvironment and by production of the catabolic product kynurenine, which selectively impairs the growth and survival of T-cells.^[6] Dysregulation of IDO1 expression is also involved in several inflammatory diseases, arthritis, and neurological disorders including Alzheimer's disease, Parkinson's disease, and cerebral ischemia.^[7]

Since IDO1 plays an important role in cancer immunotherapy and neurological diseases, searching for highly active inhibitors is now a focus of research and development efforts by pharmaceutical

COMMUNICATION

companies and academic research institutions.^[8-30] Various molecular scaffolds with inhibitory activity against IDO1 have been documented in the academic and patent literature.^[8-30] To date, several IDO1 inhibitors such as Epacadostat, PF-06840003, NLG-919 and BMS-986205 have advanced to clinical trials (Fig. 1).^[16,22,27,31,32] Indoximod (NewLink Genetics) was the first IDO1 inhibitor reported. NewLink Genetics also announced an indoximod prodrug with improved pharmacokinetic properties, but the structure has not yet been divulged.^[33] Epacadostat (Incyte, INCB024360) and Linrodostat (Bristol-Myers Squibb, BMS-986205) showed promising outcomes in phase I/II clinical trials; however, a phase III clinical trial combining Epacadostat with the PD-1 antibody pembrolizumab in melanoma failed to demonstrate efficacy.^[34] PF-06840003 (Pfizer) and NLG-919 (NewLink Genetics) also failed in phase I and II clinical trials, respectively. No IDO1 inhibitor has been approved for clinical use to date. Despite these recent clinical failures, there is a continuing need for further research into the mechanism of IDO1 in cancer biology and as a druggable target for cancer. Interest in the industrial sector in IDO1 also continues with multiple companies maintaining IDO1 inhibitors in their pipelines, chiefly for non-CNS malignancies, keeping the door open for the development of brain penetrant IDO1 inhibitors for CNS indications.

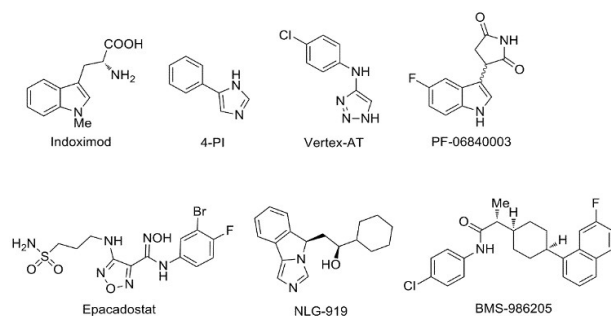


Figure 1. Representative IDO1 inhibitors

In accord with available IDO1 co-crystal structures, the IDO1 active site is structurally divided into three regions: pocket A, pocket B and a heme-cofactor.^[16,22,28,35-38] Pocket A is a narrow lipophilic pocket which is located in the distal heme site. Most inhibitors with published co-crystal structures occupy pocket A with an aromatic ring. Pocket B is near the entrance of the active site, which contains hydrophilic (Arg231) and hydrophobic (Phe226) residues. The heme cofactor structurally consists of two binding sites: the porphyrin-bound iron atom and a propionate group. Most potent inhibitors feature imidazole,^[22,25] imidazothiazole^[28] or triazole moieties^[39] tightly bound with the heme iron via an N-atom, except Epacadostat, which coordinates to the heme with an O-atom.^[27] In addition, the propionate of the heme is also a binding site which contributes to the biological activity; for example, the hydroxyl group on the side chain of NLG-919 forms a hydrogen bond with the propionate of the heme.^[22] Key interactions with the propionate of the heme were also found in Epacadostat and the imidazothiazole series.^[27,28] Through crystallographic studies of substrate-bound IDO1, a third pocket (pocket C) has been characterized, which is located below the heme plane, accounting for the inhibition by substrate phenomenon and the binding of a positive allosteric modulator of the enzyme (Phe270, Asp274 and Arg343). Interestingly, a heme-free form (holo-) of IDO1 has been also identified, wherein the three pockets form a unique and larger ligand binding pocket in which potent suicide inhibitors bind to the enzyme.^[36b,c] In contrast to other inhibitors, BMS-986205 acts as a suicide inhibitor and irreversibly inhibits hIDO1 by binding to the apo-form followed by heme release.^[34b,c]

In our previously published study we discovered a series of potent IDO1 inhibitors which structurally featured an imidazole ring connected to a phenyl ring through a C-C bond, and to an indole moiety through an *N*-CH₂ bridge (Fig. 2).^[17] Computational modeling demonstrated that the hydroxyl group interacts with Ser167 in Pocket A via a hydrogen bond, the 5-halogen substituted indole group binds in pocket B. Imidazole combines with heme iron atom and indole-NH forms interactions with the propionate of the heme by hydrogen bonding (Fig. 3). We envisaged swapping the orientation of the imidazole ring, which would allow the phenyl and indole rings to occupy the same IDO1 binding pockets as in the original orientation (Fig. 2). This modification may provide an opportunity for improving the IDO1 inhibitory activity and ADME/PK properties and producing brain penetrant compounds. In our continuous efforts to identify more potent IDO1 inhibitors, herein we report a series of 2-((1-phenyl-1H-imidazol-5-yl)methyl)-1H-indole compounds as IDO1 inhibitors.

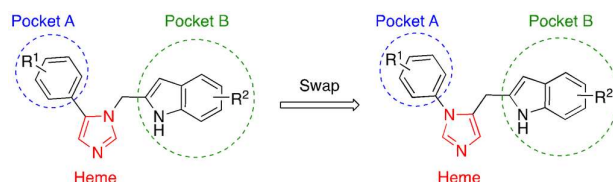


Figure 2. Design strategy for IDO1 inhibitors

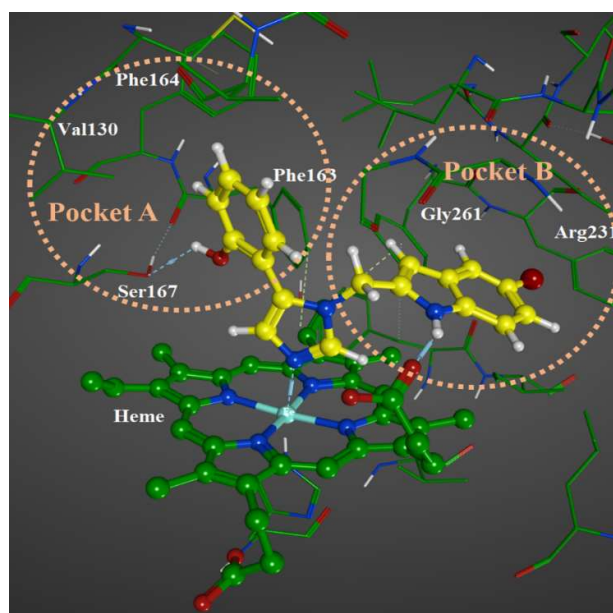


Figure 3. Computational docking for our previously reported IDO1 inhibitor (IDO1 crystal structure: PDB entry 4PK5).^[17]

Results and Discussion

Chemistry: The synthetic procedure for compounds **9a-i**, **11a-p** and **12a-d** is shown in Scheme 1. The anilines **1e** and **1q** were synthesized from 1-fluoro-2-nitrobenzene and 2-fluoro-5-chloro-1-nitrobenzene, respectively. Anilines **1a-r** and ethyl glyoxalate underwent a Van Leusen reaction to yield esters **2a-q**.^[40a, b] Reduction of esters **2a-q** with LiAlH₄ followed by oxidation with Dess-Martin periodinane provided aldehydes **3a-q**. The regioselective lithiation of *N*-Ts-indoles **4a-i** with ^tBuLi followed by nucleophilic addition to the aldehydes gave rise to the

COMMUNICATION

corresponding alcohols **5a-i** and **6a-p**. The final dehydroxylation and detosylation afforded the target molecules **9a-i** and **11a-p**. Compounds **12e-g** were prepared by deprotection of isopropyl or methyl ether groups with BCl_3 .^[40c] Compound **9j** was synthesized from **13** in three steps. Compound **13** was prepared according to the published procedure.^[41] Compound **9k** was synthesized by oxidation of **5d** followed by *N*-tosyl deprotection. Esters **16a** and **16b** were prepared by a Mitsunobu reaction of ethyl imidazole-4-carboxylate with alcohols **15a** and **15b**.^[42] The remaining steps for the preparation of **12a** and **12b** were similar those of **9a-i** and **11a-p**. Aldehydes **17a** and **17b** were synthesized from 2- and 3-iodothiophene according to published procedures.^[41] The remaining steps for the preparation of **12c** and **12d** were similar as that for preparation of **9a-i** and **11a-p**.

The syntheses of **10a-h** are shown in Scheme 2. A Horner-Wadsworth-Emmons reaction between **3a** and **19** afforded **10a**. Reductive amination of aldehyde **3a** and secondary amines **20a-d** provided **10b-e**. Coupling of secondary amines **21a-c** with Boc-glycine and further deprotection of *tert*-butyloxycarbonyl group provided **22a-c**. Compounds **22a-c** reacted with isothiocyanate **23** to give the thiourea **24a-c**. Selective methylation of **24a-c** and subsequent cyclization of **25a-c** with Lawesson's reagent afforded **26a-c**. Final removal of SMe group of **26a-c** with nickel Raney gave **10f-h**.^[43]

Structure-activity relationship studies: We first examined a series of substituted indole moieties to investigate the effect of indole ring substitution on potency (Table 1). The determination of IC_{50} and EC_{50} values is described in Supporting Information 4.2 and 4.3. Compound **9a** with a non-substituted indole moiety has an IC_{50} of $16 \mu\text{M}$. We explored whether substituents on the indole ring would increase the potency by either forming interactions with Arg231 or hydrophobic interactions with additional residues in pocket B. Compounds containing 4- or 6-chloro indole moieties (**9b** and **9c**) did not produce a significant change in IDO1 inhibition ($\text{IC}_{50} = 11$ and $22.15 \mu\text{M}$, respectively) relative to **9a** ($\text{IC}_{50} = 16.12$). Compared with **9a-c** ($\text{IC}_{50} = 16.12$, 11.77 and $22.15 \mu\text{M}$ respectively), the IC_{50} of **9d** was improved to $0.44 \mu\text{M}$ ($\text{EC}_{50} = 0.85 \mu\text{M}$) by introducing a chloro group on C5-position of the indole. This can be rationalized by the the chlorine acting as both a halogen bond donor and hydrogen bond acceptor with Arg231 in pocket B (Fig. 4).^[43a] This result was consistent with published results which demonstrated that π -cation interaction between chloro group and Arg231 is important for IDO inhibitory activity.^[17,19,28] Other functional groups on the C5-position of indole were also investigated: compound **9e** containing 5-bromo caused a slight loss of activity ($\text{IC}_{50} = 0.46 \mu\text{M}$, $\text{EC}_{50} = 1.9 \mu\text{M}$). However, fluoro, cyano, methoxy and methyl groups (**9f-i**) caused a slight decrease in activity relative to **9d** with IC_{50} values ranging from 2.9 to $8.7 \mu\text{M}$. A further loss of activity ($\text{IC}_{50} = 28 \mu\text{M}$) was observed for **9j** when the CH_2 bridge was switched from C2-position to C3-position of the indole ring. Replacement of CH_2 linker with a ketone group led to a complete loss of activity for **9k**, probably because of the electron pair repulsion created between the carbonyl oxygen's lone pair of **9k** and the propionate of the heme which may cause a decrease in the binding efficiency.^[23] In addition, several replacements of indole ring with heterocycles were attempted. However, replacement of indole with pyrrolidine-2,5-dione (**10a**, $\text{IC}_{50} > 200 \mu\text{M}$), anilines (**10b** and **10c**, $\text{IC}_{50} = 53.61$ and $82.3 \mu\text{M}$ respectively) and tetrahydroisoquinoline (**10d** and **10e**, $\text{IC}_{50} > 200$ and $200 \mu\text{M}$ respectively) led to a significant drop in IDO1 inhibition activities compared with **9d** ($\text{IC}_{50} = 0.44 \mu\text{M}$, $\text{EC}_{50} = 0.85 \mu\text{M}$). Considering that the basicity of the ligand is crucial to form a metal complex, increasing the basicity of the imidazole may result in a stronger binding to the heme iron of IDO1, which may improve IDO1 inhibitory activity from bottom. To increase the basicity of the imidazole, a *N*-atom was introduced at the C5-position of imidazole ring (**10f-h**). Compared with **10d** ($\text{IC}_{50} > 200 \mu\text{M}$) and **10e** ($\text{IC}_{50} > 200 \mu\text{M}$), compounds **10f-h** displayed improved IDO1 inhibitory activities with IC_{50} of 1.24 to $8.4 \mu\text{M}$, respectively, but were less potent than **9d** ($\text{IC}_{50} = 0.44 \mu\text{M}$, $\text{EC}_{50} = 0.85 \mu\text{M}$).

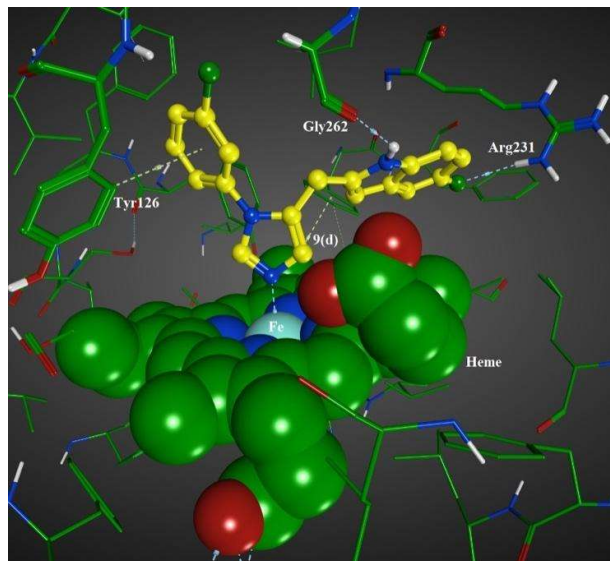
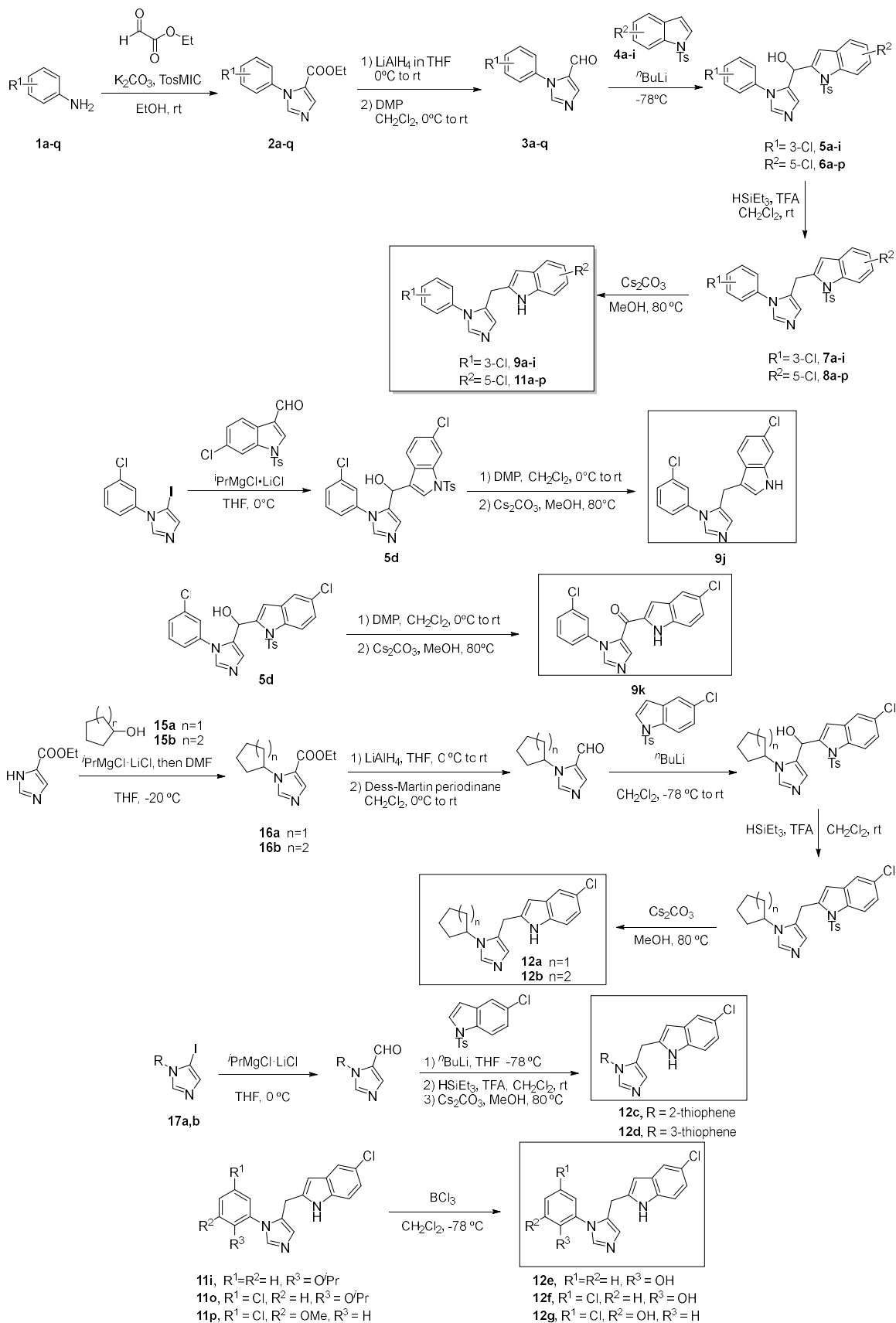


Fig. 4. Computational docking of **9d** (IDO1 crystal structure: PDB entry 4PK5).

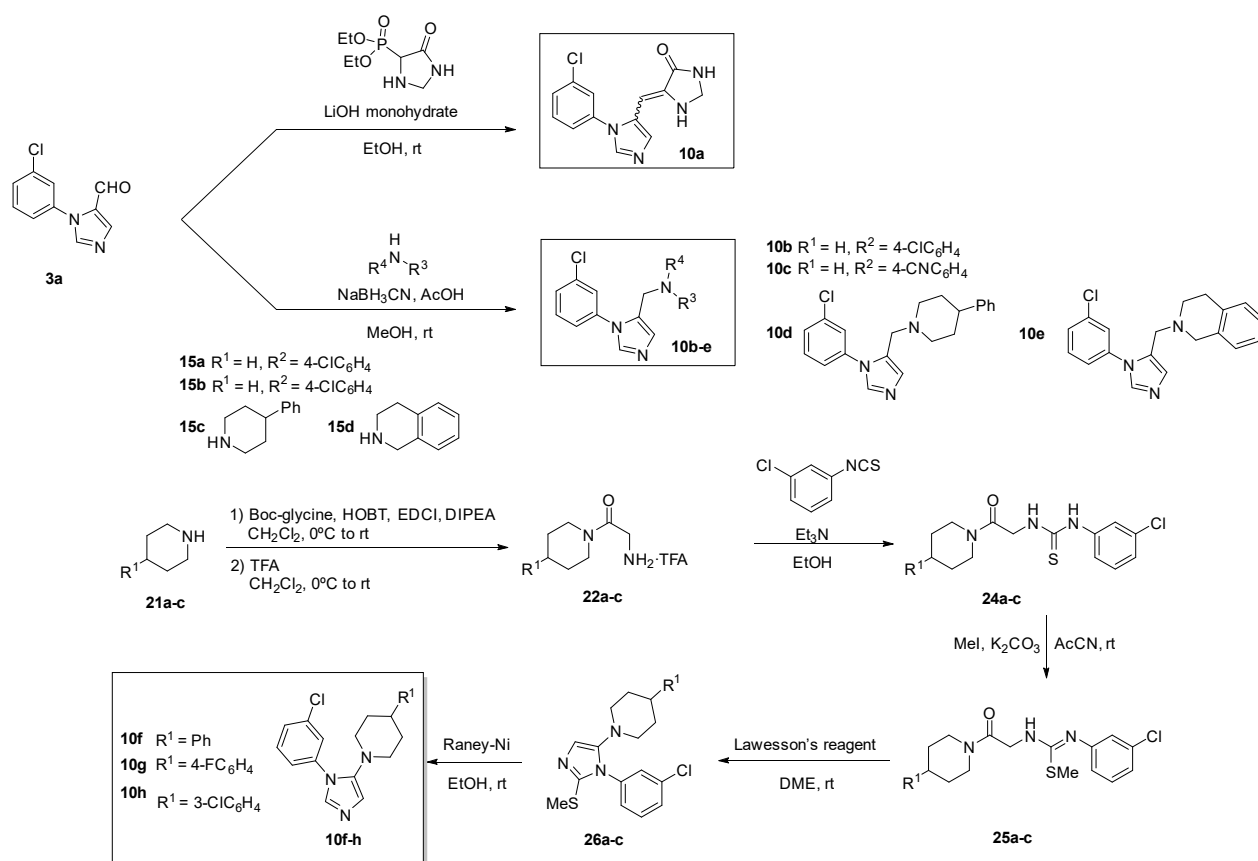
Next, we attempted to optimize the phenyl ring in pocket A (Table 2). The unsubstituted phenyl compound **11a** had an IC_{50} of $90 \mu\text{M}$. To improve IDO1 inhibitory activity substitutions on the phenyl ring were investigated. *Ortho*-substituted phenyl groups (**11b-e**) had poor activity with IC_{50} values between 10 and $200 \mu\text{M}$. Switching the substitution from the *ortho*- to *para*-position did not produce any improvement in activity (**11f-h**). Surprisingly, *meta*-substituted phenyl yielded more potent compounds (**9d**, **11i**). Compounds **9d** and **11i** have IC_{50} values of 0.44 and $0.98 \mu\text{M}$, respectively. *Meta*-substitution may be the optimal position to occupy the small lipophilic cavity at the top of pocket A and, at the same time, generate an interaction between the sulfur atom of Cys129 and the chlorine of the 3-chlorophenyl moiety.^[11,17,25] The 3-F, 3-OMe substitutions produced compounds with IC_{50} values greater than $10 \mu\text{M}$ (**11j** and **11k**). We next studied the influence of di-substituted groups on phenyl rings and found di-substituted compounds **11l-n** displaying decreased IDO inhibitory activities ($\text{IC}_{50} > 4.9 \mu\text{M}$), compared with most potent mono-substituted compound **9d**. We then explored replacement of the phenyl functionality with aliphatic and heterocyclic substituents and observed that compound **12a**, containing the cyclopentyl moiety, had an IC_{50} of $45 \mu\text{M}$ ($\text{EC}_{50} = 0.7 \mu\text{M}$). It is hypothesized this phenomenon arises due to complications in regulating the IDO1 redox activity and/or an environmental effect, which likely also accounts for the reported lower EC_{50} values as compared to the IC_{50} values in the cell-based activity assay.^[44] As we discussed above, a 3-halogen phenyl ring is necessary to maintain the activity by establishing interactions with the amino acid residues in pocket A. The cyclopentyl ring in **12a** cannot interact with residues in pocket A, which may be the cause of reduced potency. Changing from a cyclopentyl to cyclohexyl ring in pocket A led to an inactive compound (**12b**, $\text{IC}_{50} > 200 \mu\text{M}$). Replacements of phenyl with a thiophene led to a loss activity (**12c**, $\text{IC}_{50} = 60 \mu\text{M}$ and **12d**, $\text{IC}_{50} = 18 \mu\text{M}$).

Based on our previous results and literature precedent, IDO1 inhibitory activity can be increased by the introduction of a hydroxyl group at the *ortho*-position of the phenyl ring.^[17,23,25] The hydroxyl group is thought to interact with Ser167 in the pocket A through a hydrogen bond, which contributes to the inhibitory activity. Inspired by this observation, we installed a 2-hydroxyl group on the phenyl ring of **11a** to produce compound **12e** and as

COMMUNICATION

Scheme 1. Synthetic routes of **9a-i**, **11a-p** and **12a-g**.

COMMUNICATION

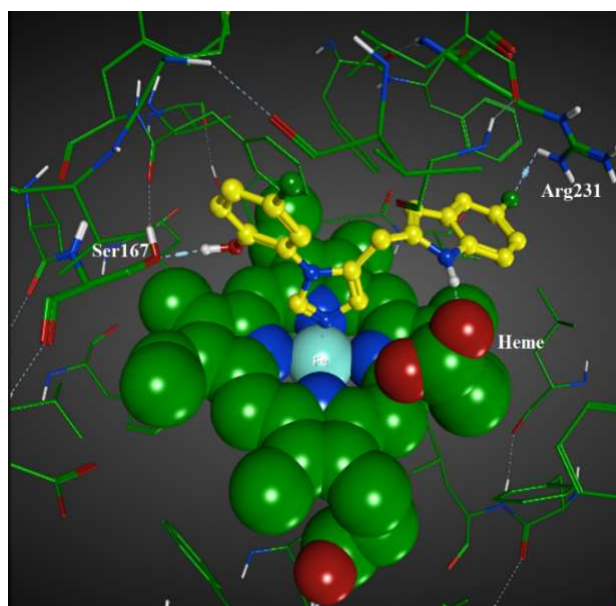


Scheme 2. Synthetic routes of 10a-h.

predicted, it displayed a significantly improved IC_{50} of 2.29 μM , compared with the non-hydroxyl compound **11a** (IC_{50} = 90 μM). Encouraged by this result, we further explored whether inclusion of an additional substituent on the phenyl ring of **12e** would substantially improve binding affinity. A 3-chloro group was found to be the best substituent in pocket A for IDO1 inhibitory potency (**9d**). **12f** was synthesized by installing a 3-chloro group on the phenyl ring of **12e**. Significantly, **12f** displayed an inhibitory activity of 0.16 μM , approximately 2.8-fold more potent than **9d**, with an EC_{50} of 0.3 μM . Further switching from a 2-hydroxyl to 3-hydroxyl group (**12g**) led to decreased activity (IC_{50} = 1.45 μM), which suggested that the 2-hydroxyl group played an important role in maintaining IDO1 inhibitory activity.^[17,25,39] The SAR studies of di-substituted compounds indicated that both a 2-hydroxyl and 5-chloro in Pocket A (**12f**) are necessary for potent IDO inhibition, and other di-substituted compounds (**11i-n**) showed decreased IDO inhibitory activities.

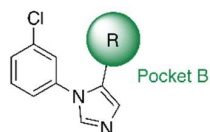
The binding modes of potent compounds **9d** and **12f** with IDO1 were further evaluated by computational modelling. As shown in Fig. 4, computational modelling of **9d** reveals that the *N1*-phenyl ring likely occupies pocket A, and the indole ring extends to pocket B. The imidazole ring coordinates with the heme iron *via* an *N*-atom. The binding model of **12f** was similar with that of **9d**. Computational modeling of **12f** (Fig. 5) further suggests that the 2-hydroxyphenyl group fits in pocket A and the hydroxyl group acts as a hydrogen bond donor to Ser167, which may account for the high potency against IDO1. The indole-NH was found to interact with the propionate of the heme through a

hydrogen bond. The interaction with propionate of the heme was found to be important for the IDO inhibitory activity.^[17,22,27,28]

Fig. 5. Computational docking of **12f** (IDO1 crystal structure: PDB entry 4PK5).^[17]

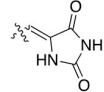
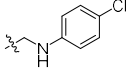
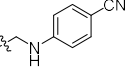
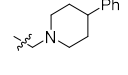
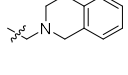
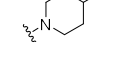
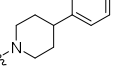
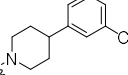
COMMUNICATION

Table 1. SAR studies of pocket B.



Compound	R	IC ₅₀ (μM)	EC ₅₀ (μM)	ClogP	LE ^[a]	BBB Score ^[b]	GBVI/WSA dG docking Score (kcal/mol)
9a		16.12		4.63	0.31	4.24	-8.4039
9b		11.77		5.51	0.30	4.18	-8.5461
9c		22.15	10.0	5.51	0.30	4.18	-8.7656
9d		0.44	0.85	5.51	0.39	4.18	-8.9499
9e		0.46	1.90	5.51	0.39	4.13	-8.9346
9f		2.90	3.34	5.66	0.34	4.2	-8.5877
9g		2.32	2.12	4.45	0.33	4.11	-9.2024
9h		8.67	1.66	4.88	0.30	4.31	-9.1466
9i		2.57	>10	5.36	0.34	4.2	-8.9140
9j		26.86	>2.50	5.51	0.28	4.19	-8.5745
9k		>200		5.24		3.94	-8.4426

COMMUNICATION

10a		200		1.92		4.07	-7.2551
10b		53.61	>10	4.77	0.28	4.98	-8.2282
10c		82.3		3.89	0.26	4.67	-8.6985
10d		>200		5.24		4.95	-7.3541
10e		>200		4.69		4.97	-8.1877
10f		1.24	>2.50	5.60	0.35	4.94	-8.8333
10g		1.30	>2.50	5.74	0.33	4.89	-9.1090
10h		8.40		6.31	0.28	4.88	-7.5222

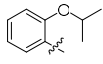
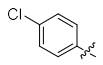
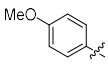
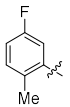
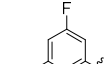
The cellular assay that was employed can be found in the 4.3 section of the Supporting Information. [a] Ligand efficiency (LE) calculated using IDO1 IC₅₀. [b] BBB Score calculated according to Ref [49].

Table 2. SAR studies of pocket A.



Compound	R	IC ₅₀ (μM)	EC ₅₀ (μM)	ClogP	LE ^[a]	BBB Score ^[b]	GBVI/WSA dG docking Score (kcal/mol)
11a		90.31		5.01	0.26	4.24	-8.4455
11b		144.6		5.74	0.23	4.17	-9.0412
11c		156.1		4.94	0.23	4.19	-8.4820

COMMUNICATION

11d		10.07		4.83	0.29	4.36	-9.3821
11e		>200		5.66		4.23	-7.7936
11f		58.66		5.51	0.26	4.18	-8.3626
11g		>200		4.94		4.31	-8.4238
11h		45.74		4.82	0.25	4.2	-8.9892
11i		0.98	7.20	5.89	0.37	4.13	-9.2475
11j		12.85		4.94	0.30	4.2	-8.6657
11k		25.90	>2.5	4.82	0.27	4.31	-9.3143
11l		114.0		5.44	0.23	4.16	-9.1159
11m		4.85		6.34	0.31	4.12	-8.6350
11n		34.40		4.99	0.25	4.27	-8.367
12a		44.81	0.71	4.39	0.30	4.8	-8.998
12b		>200		4.95		4.77	-7.898

COMMUNICATION

12c		60.0		4.69	0.28	4.22	-7.989
12d		18.22	>2.5	4.69	0.32	4.24	-8.321
12e		2.29	0.64	4.44	0.36	4.22	-9.001
12f		0.16	0.30	5.21	0.40	4.21	-9.206
12g		1.45	> 2.5	5.21	0.36	4.29	-8.739

The cellular assay that was employed can be found in the 4.3 section of the Supporting Information. [a] Ligand efficiency (LE) calculated using IDO1 IC₅₀. [b] BBB Score calculated according to Ref [49].

Table 3. Pharmacokinetic parameters of compounds **9d** and **12f**. PO dose was administered at 5 mg/kg and IV dose was administered at 2.5 mg/kg.

Parameter	9d				12f			
	IV		PO		IV		PO	
	Plasma	Brain	Plasma	Brain	Plasma	Brain	Plasma	Brain
R ² _{adj}	0.94	0.93	0.98	0.96	0.96	0.98	0.87	0.75
C _{max} (ng/mL or g)	1,233	4,825	235	1,114	1,251	269	135	50
T _{max} (h)	-	-	0.5	0.5	-	-	0.5	2
T _{1/2} (h)	1.0	0.9	1.9	1.4	1.8	2.2	2.1	14.0
V _{dss} (L)	3.4	0.6	-	-	5.2	8.3	-	-
Cl (mL/min/kg)	3.7	0.5	2.4	2.2	4.1	2.2	3.6	20.7
T _{Last}	6	6	6	8	8	8	8	8
AUC _{0-Tlast} (ng·h/mL or g)	666	5,023	357	2,115	593	1,032	318	324
AUC _{0-∞}	675	5,118	395	2,171	608	1,159	342	1,042
MRT _{0-Tlast} (h)	0.84	1.05	-	-	1.03	2.93	-	-
Oral Bioavailability (%)	29	-	-	-	28	-	-	-
AUC _{0-Tlast} Brain/Plasma	7.5		5.9		1.7		1.0	

Selected potent compounds (**9c-i**, **11n**, **12a**, **12c-f**) were advanced to solubility and in vitro intrinsic clearance CL_{int} using mouse liver microsomes (MLM) studies (**9f-h**, **11n**, **12a**, **12e-f**). Non-hydroxyl compounds, **9d-f** bearing a 5-halogen in Pocket B had low solubility (K_{sol} < 10 μM). The solubility for **9c** (6-Cl) and **9g-i** (5-CN, 5-OMe, 5-Me) were improved with K_{sol} values ranging from 10 to 31.2 μM. Compounds containing an aliphatic ring (**12a**) and heterocycle (**12c** and **d**) in Pocket A exhibited poor solubility (K_{sol} < 1.2 μM), likely due to high lipophilicity. The phenolic compound **12e** had good solubility with K_{sol} = 28 μM possibly because the hydroxyl group increases hydrophilicity. The

most potent compound **12e** displayed improved solubility with K_{sol} = 9.38 μM.

9f-h resulted in high MLM clearance (CL_{int} > 348 mL/min/kg) possibly because of high lipophilicity. Compound **12a** had poor MLM stability (CL_{int} = 1337 mL/min/kg), possibly due to poor metabolic stability of the cyclohexyl group as first pass metabolism of cycloalkyl groups is a well-documented issue.^[23] The phenolic compound **12e** had MLM data with CL_{int} = 319 mL/min/kg, whilst **12f** showed acceptable MLM data (31.7 mL/min/kg). Compounds **9d** and **12f** were also assayed for brain protein binding *via* equilibrium dialysis (percentage bound = 98.29 and 99.92% respectively). The high protein binding percentages

COMMUNICATION

for **9d** and **12f** also arose from the high lipophilicity of these compounds.^[17]

We calculated the LE for our compounds (Tables 1 and 2) to assess whether they are in the appropriate range for druglike compounds ($LE > 0.3$). The most potent compound, **12f**, displayed the best LE value (0.4), which is comparable to the mean LE value (0.45) for most approved drugs administered orally.^[45] The 'GBVI/WSA dG' docking scores^[46a] for our compounds are given in Table 1 and 2 to estimate the binding affinity of each ligand in the active site of IDO1. We can see that most of the active compounds, including **9d** and **12f**, have low GBVI/WSA binding free energy. Detailed information of docking simulations protocols, ligand structure optimization, dataset curation and descriptor calculation has been given in supporting information and in prior publications.^[46b-d] There are several potential applications for a brain penetrant IDO1 inhibitor.^[16,45,47] To evaluate our compounds for their ability to penetrate the brain, we used two assessment tools, one called the Brain Exposure Efficiency (BEE) score, and the other called the Blood Brain Barrier (BBB) score; both developed by our group.^[48,49] The BBB score estimates passive diffusion across the BBB, whereas the BEE score predicts active transport across the BBB as a function of efflux and influx transporters. The BBB score values of our active compounds ranged between 4 to 5, which is optimal for BBB penetration. The BBB scores for **9d** and **12f** are 4.18 and 4.21 respectively, which predict a good brain penetration for these analogs. The BBB scores for all other analogs are presented in Tables 1 and 2, respectively. The predicted $K_{p,uu}$ values (the BEE scores) for both **9d** and **12f** are above 0.10, which is optimal for brain penetration.^[49] The BEE Score efflux and influx transporter activity calculations predicts that the analog **9d** is predicted to be a substrate of OCT1 influx transporter and **12f** is predicted to be a substrate of both OCT1 and OCT2 influx transporters. Compound **9d** is predicted not to be a substrate of either the P-gp or BCRP efflux transporters. More details about these BEE calculations are provided in supporting information Tables S1-S6. Brain penetration and transporter affinity predictions could be employed for further studies in CNS drug development. Based on the above results we examined the pharmacokinetic profiles of compounds **9d** and **12f**.

Our pharmacokinetic studies on **9d** and **12f** (Fig.6; Table 3) demonstrated that both compounds were reasonably brain penetrant ($AUC_{Brain/Plasma} > 1$) but that both compounds had somewhat low oral bioavailability (< 30%). The brain exposure of **9d** was several fold that of **12f** ($AUC_{0-Tlast Brain} = 2115, 324$ for **9d** and **12f**, respectively) The 2-hydroxyl group in **12f** decreases lipophilicity and increase the number of hydrogen bond donors relative to **9d**, which may explain its lower brain exposure relative to **12f**. Additionally, we attribute the short half-lives of the compounds to possible oxidation of the methylene between the imidazole and indole on the pocket B side, or, oxidation of the chlorobenzene or phenol on the pocket A side of **9d** and **12f** respectively.^[50]

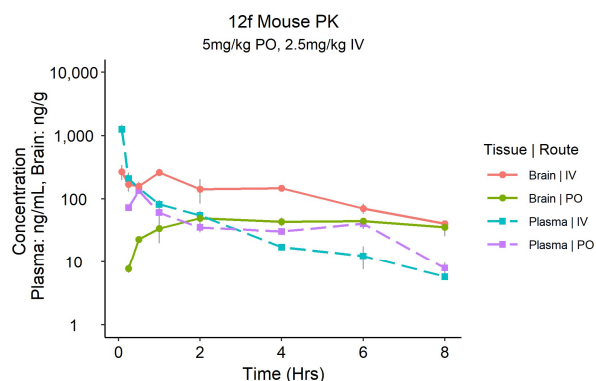
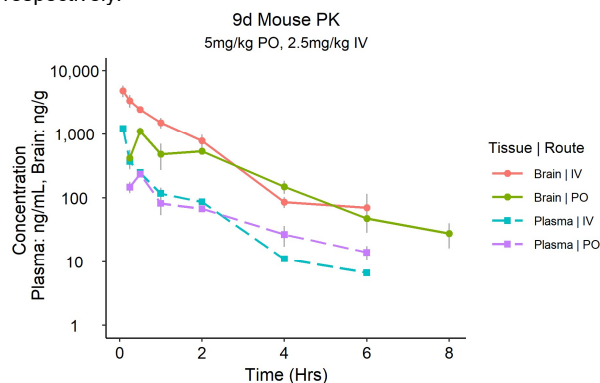


Fig. 6. Pharmacokinetic profiles of Compounds **9d** and **12f**. A) Mice were administered **9d** 5mg/kg PO and 2.5 mg/kg IV. Brain and plasma were collected at each indicated time point and concentration of the compound was determined. B) Mice were administered **12f** 5mg/kg PO and 2.5 mg/kg. Brain and plasma were collected at each indicated time point and concentration of the compound was determined. Full PK parameters for each compound are presented in Table 3.

Conclusion

In summary, on the basis of computational docking simulations, a series of 2-((1-phenyl-1*H*-imidazol-5-yl)methyl)-1*H*-indoles was designed, synthesized, and evaluated as IDO1 inhibitors. Optimization of pocket A and B substituents led to identification of compound **12f** as our most potent IDO1 inhibitor. A structure activity relationship analysis indicated that a 5-chloro group on the indole ring is essential for the IDO1 inhibitory activity in pocket B. Both the 3-chloro and 2-hydroxyl groups on the phenyl ring are important for the IDO1 inhibitory activity targeting pocket A. Computer docking studies demonstrated that the hydroxyl group may interact with the Ser167 residue in pocket A. Potent compounds **9d** and **12f** were predicted to have good brain penetrance as calculated by the BBB score and BEE score. We then performed a pharmacokinetic study, which demonstrated that **9d** and **12f** were both brain penetrant, though they had relatively low exposure and half-lives. The scaffold we have developed could be further developed to produce brain penetrant IDO1 inhibitor compounds for CNS indications, such as neuro-oncology or Alzheimer's disease. Towards this goal, studies on the replacement of the 2-hydroxyl group with other H-donors, which may enhance both IDO1 inhibitory activity and ADME/PK properties (such as solubility, MLM and PK), are ongoing in our laboratory.

Acknowledgements

This work was supported by a CIHR operating grant and by funding from the Krembil Foundation. DFW acknowledges salary support from a Canada Research Chair, Tier 1. We thank Dr. Christopher J. Barden and Dr. Jake Goodwin-Tindall for helpful discussions.

Keywords: IDO1 inhibitors • imidazole • structure-activity relationship • computational modelling •

- [1] D. N. Khalil, E. L. Smith, R. J. Brentjens, J. D. Wolchok, *Nat. Rev. Clin. Oncol.* **2016**, *13*, 273-290.
- [2] I. Mellman, G. Coukos, G. Dranoff, *Nature*, **2011**, *480*, 480-489.
- [3] H. Sugimoto, S. Oda, T. Otsuki, T. Hino, T. Yoshida, Y. Shiro, *Proc. Natl. Acad. Sci. U. S. A.* **2006**, *103*, 2611-2616.
- [4] A. B. Dounay, J. B. Tuttle, P. R. Verhoest, *J. Med. Chem.* **2015**, *58*, 8762-8782.
- [5] G. C. Prendergast, C. Smith, S. Thomas, L. Mandik-Nayak, L. Laury-Kleintop, R. Metz, A. J. Muller, *Cancer Immunol. Immunother.* **2014**, *63*, 721-735.

COMMUNICATION

- [6] J. Godin-Ethier, L. A. Hanafi, C. A. Piccirillo, R. Lapointe, *Clin. Cancer Res.* **2011**, *17*, 6985–6991.
- [7] L. Vécsei, L. Szalárdy, F. Fülöp, J. Toldi, *Nat. Rev. Drug Discovery*, **2013**, *12*, 64–82.
- [8] T. Weng, X. Qiu, J. Wang, Z. Li, J. Bian, *Eur. J. Med. Chem.* **2018**, *143*, 656–669.
- [9] X. Wang, S. Sun, Q. Dong, X. Wu, W. Tang, Y. Xing, *MedChemComm* **2019**, *10*, 1740–1754.
- [10] M. Sono, S. G. Cady, *Biochemistry*, **1989**, *28*, 5392–5399.
- [11] S. Fallarini, A. Massarotti, A. Gesù, S. Giovarruscio, G. Coda Zabetta, R. Bergo, B. Giannelli, A. Brunco, G. Lombardi, G. Sorba and T. Pirali, *MedChemComm* **2016**, *7*, 409–419.
- [12] J. A. C. Alexandre, M. K. Swan, M. J. Latchem, D. Boyall, J. R. Pollard, S. W. Hughes, J. Westcott, *ChemBioChem* **2018**, *19*, 552–561.
- [13] S. Y. Lin, T. K. Yeh, C. C. Kuo, J. S. Song, M. F. Cheng, F. Y. Liao, M. W. Chao, H. L. Huang, Y. L. Chen, C. Y. Yang, M. H. Wu, C. L. Hsieh, W. Hsiao, Y. H. Peng, J. S. Wu, L. M. Lin, M. Sun, Y. S. Chao, C. Shih, S. Y. Wu, S. L. Pan, M. S. Hung, S. H. Ueng, *J. Med. Chem.* **2016**, *59*, 419–430.
- [14] W. P. Malachowski, M. Winters, J. B. DuHadaway, A. Lewis-Ballester, S. Badir, J. Wai, M. Rahman, E. Sheikh, J. M. LaLonde, S. R. Yeh, G. C. Prendergast, A. J. Muller, *Eur. J. Med. Chem.* **2016**, *108*, 564–576.
- [15] S. Paul, A. Roy, S. J. Deka, S. Panda, V. Trivedi, D. Manna, *Eur. J. Med. Chem.* **2016**, *121*, 364–375.
- [16] S. Crosignani, P. Bingham, P. Bottemanne, H. Cannelle, S. Cauwenberghs, M. Cordonnier, D. Dalvie, F. Deroose, J. L. Feng, B. Gomes, S. Greasley, S. E. Kaiser, M. Kraus, M. Negrerie, K. Maegley, N. Miller, B. W. Murray, M. Schneider, J. Solowij, A. E. Stewart, J. Tumang, V. R. Torti, B. Van Den Eynde, M. Wythes, *J. Med. Chem.* **2017**, *60*, 9617–9629.
- [17] M. G. Brant, J. Goodwin-Tindall, K. R. Stover, P. M. Stafford, F. Wu, A. R. Meek, P. Schiavini, S. Wohnig, D. F. Weaver, *ACS Med. Chem. Lett.* **2018**, *9*, 131–136.
- [18] K. Fang, G. Dong, Y. Li, S. He, Y. Wu, S. Wu, W. Wang, C. Sheng, *ACS Med. Chem. Lett.* **2018**, *9*, 312–317.
- [19] Y. Zou, F. Wang, Y. Wang, Q. Sun, Y. Hu, Y. Li, W. Liu, W. Guo, Z. Huang, Y. Zhang, Q. Xu, Y. Lai, *Eur. J. Med. Chem.* **2017**, *140*, 293–304.
- [20] A. Coluccia, S. Passacantilli, V. Famigliini, M. Sabatino, A. Patsilinos, R. Ragno, C. Mazzoccoli, L. Sisinni, A. Okuno, O. Takikawa, R. Silvestri, G. La Regina, *J. Med. Chem.* **2016**, *59*, 9760–9773.
- [21] K. Fang, S. Wu, G. Dong, Y. Wu, S. Chen, J. Liu, W. Wang, C. Sheng, *Org. Biomol. Chem.* **2017**, *15*, 9992–9995.
- [22] Y. H. Peng, S. H. Ueng, C. T. Tseng, M. S. Hung, J. S. Song, J. S. Wu, F. Y. Liao, Y. S. Fan, M. H. Wu, W. C. Hsiao, C. C. Hsueh, S. Y. Lin, C. Y. Cheng, C. H. Tu, L. C. Lee, M. F. Cheng, K. S. Shia, C. Shih, S. Y. Wu, *J. Med. Chem.* **2016**, *59*, 282–293.
- [23] S. Kumar, J. P. Waldo, F. A. Jaipuri, A. Marcinowicz, C. Van Allen, J. Adams, T. Kesharwani, X. Zhang, R. Metz, A. J. Oh, S. F. Harris, M. R. Mautino, *J. Med. Chem.* **2019**, *62*, 6705–6733.
- [24] S. Chen, W. Guo, X. Liu, P. Sun, Y. Wang, C. Ding, L. Meng, A. Zhang, *Eur. J. Med. Chem.* **2019**, *179*, 38–55.
- [25] a) S. Kumar, D. Jaller, B. Patel, J. M. LaLonde, J. B. DuHadaway, W. P. Malachowski, G. C. Prendergast, A. J. Muller, *J. Med. Chem.* **2008**, *51*, 4968–4977; b) Y-H. Peng, F-Y. Liao, C-T. Tseng, R. Kuppusamy, A-S. Li, C-H. Chen, Y-S. Fan, S-Y. Wang, M-H. Wu, C-C. Hsueh, J-Y. Chang, L-C. Lee, C. Shih, K-S Shia, T-K. Yeh, M-S. Hung, C-C. Kuo, J-S. Song, S-Y. Wu, S-H. Ueng *J. Med. Chem.* **2020**, *63*, 4, 1642–1659.
- [26] W. Tu, F. Yang, G. Xu, J. Chi, Z. Liu, W. Peng, B. Hu, L. Zhang, H. Wan, N. Yu, F. Jin, Q. Hu, L. Zhang, F. He, W. Tao, *ACS Med. Chem. Lett.* **2019**, *10*, 949–953.
- [27] E. W. Yue, R. Sparks, P. Polam, D. Modi, B. Douty, B. Wayland, B. Glass, A. Takvorian, J. Glenn, W. Zhu, M. Bower, X. Liu, L. Leffert, Q. Wang, K. J. Bowman, M. J. Hansbury, M. Wei, Y. Li, R. Wynn, T. C. Burn, H. K. Koblish, J. S. Fridman, T. Emm, P. A. Scherle, B. Metcalf, A. P. Combs, *ACS Med. Chem. Lett.* **2017**, *8*, 486–491.
- [28] S. Tojo, T. Kohno, T. Tanaka, S. Kamioka, Y. Ota, T. Ishii, K. Kamimoto, S. Asano, Y. Isobe, *ACS Med. Chem. Lett.* **2014**, *5*, 1119–1123.
- [29] Q. Du, X. Feng, Y. Wang, X. Xu, Y. Zhang, X. Qu, Z. Li, J. Bian, *Eur. J. Med. Chem.* **2019**, *182*, 111629.
- [30] S. Cai, X. Yang, P. Chen, X. Liu, J. Zhou, H. Zhang, *Bioorganic Chemistry*, **2020**, *94*, 103356.
- [31] G. L. Beatty, P. J. O'Dwyer, J. Clark, J. G. Shi, K. J. Bowman, P. A. Scherle, R. C. Newton, R. Schaub, J. Maleski, L. Leopold, T. F. Gajewski, *Clin. Cancer Res.* **2017**, *23*, 3269.
- [32] J. E. Cheong, A. Ekkati, L. Sun, *Expert Opin. Ther. Pat.* **2018**, *28*, 317–330.
- [33] M.R. Mautino, S. Kumar, H. Zhuang, J. Waldo, F. Jaipuri, H. Potturi, E. Brincks, J. Adams, A. Marcinowicz, C. Van Allen, N. Vahanian, C. J. Link, *Cancer Res.* **2017**, *77*, 4076.
- [34] a) V. G. Long, R. Dummer, O. Hamid, T. F. Gajewski, C. Caglevic, S. Dalle, A. Arance, M. S. Carlino, J.-J. Grob, T. M. Kim, L. Demidov, C. Robert, J. Larkin, J. R. Anderson, J. Maleski, M. Jones, S. J. Dieder, T. C. Mitchell, *Lancet Oncol.* **2019**, *20*, 1083–1097. b) M. T. Nelp, P. A. Kates, J. T. Hunt, J. A. Newitt, A. Balog, D. Maley, X. Zhu, L. Abell, A. Allentoff, R. Borzilleri, H. A. Lewis, Z. Lin, S. P. C. Seitz, J. T. Yan, Groves, *Proc. Natl. Acad. Sci. U.S.A.* **2018**, *115*, 3249–3254. c) K. N. Pham, S.-R. Yeh, *J. Am. Chem. Soc.* **2018**, *140*, 14538–14541.
- [35] U. F. Röhrig, L. Awad, A. Grosdidier, P. Larrieu, V. Stroobant, D. Colau, V. Cerundolo, A. J. Simpson, P. Vogel, B. J. Van den Eynde, V. Zoete, O. Michielin, *J. Med. Chem.* **2010**, *53*, 1172–118.
- [36] U. F. Röhrig, A. Reynaud, Somi Reddy Majjigapu, P. Vogel, Florence Pojer, V. Zoete, *J. Med. Chem.* **2019**, *62*, 8784–8795. b) A. Coletti, M. Ballarotto, A. Riccio, A. Carotti, U. Grohmann, E. Camaioni, A. Macchiarulo, *ChemMedChem* **2020**, *15*, 891–899. c) A. Lewis-Ballester, K. N. Pham, D. Batabyal, S. Karkashon, J. B. Bonanno, T. L. Poulos, S.-R. Yeh, *Nature Commun.* **2017**, *8*, 1693.
- [37] H. Zhang, K. Liu, Q. Pu, A. Achab, M. J. Ardolino, M. Cheng, Y. Deng, A. C. Doty, H. Ferguson, X. Fradera, I. Knemeyer, R. Kurukulasuriya, Y. Lam, C. A. Lesburg, T. A. Martinot, M. A. McGowan, J. R. Miller, K. Otte, P. J. Biju, N. Sciammetta, N. Solban, W. Yu, H. Zhou, X. Wang, D. J. Bennett, Y. Han, *ACS Med. Chem. Lett.* **2019**, *10*, 1530–1536.
- [38] K. N. Pham, A. Lewis-Ballester, S. Yeh, *J. Am. Chem. Soc.* **2019**, *141*, 18771–18779.
- [39] U. F. Röhrig, S. R. Majjigapu, A. Grosdidier, S. Bron, V. Stroobant, L. Pilotte, D. Colau, P. Vogel, B. J. Van den Eynde, V. Zoete, O. Michielin, *J. Med. Chem.* **2012**, *55*, 5270–5290.
- [40] a) A. M. Van Leusen, J. Wildeman, O. H. Oldenziel, *J. Org. Chem.* **2012**, *42*, 1153–1159. b) B. Chen, M. S. Bednarz, R. Zhao, J. E. Sundeen, P. Chen, Z. Shen, A. P. Skoumbourdis, J. C. Barrish, *Tetrahedron Lett.* **2000**, *41*, 5453–5456. c) A. V. Kalinin, M. A. Reed, B. H. Norman, V. Snieckus, *J. Org. Chem.* **2003**, *68*, 5992–5999.
- [41] Y. Wu, S. Izquierdo, P. Vidossich, A. Lledys, A. Shafir, *Angew. Chem. Int. Ed.* **2016**, *55*, 7152–7156.
- [42] J. K. Laha, G. D. Cuny, *J. Org. Chem.* **2011**, *76*, 8477–8482.
- [43] a) C. Lamberth, R. Dumeunier, S. Trah, S. Wendeborn, J. Godwin, P. Schneider, A. Corran, *Bioorg. Med. Chem.* **2013**, *21*, 127–134. b) S. Panda, A. Roy, S. J. Deka, V. Trivedi, D. Manna, *ACS Med. Chem. Lett.* **2016**, *7*, 12, 1167–1172.
- [44] A. L. Hopkins, G. M. Keseru, P. D. Leeson, D. C. Rees, C. H. Reynolds, *Nat. Rev. Drug Discovery* **2014**, *13*, 105–121.
- [45] E. Fertan, K. R. J. Stover, M. G. Brant, P. M. Stafford, B. Kelly, E. Diez-Cecilia, A. A. Wong, D. F. Weaver, R. E. Brown, *Front. Pharmacol.* **2019**, *24*, 1044.
- [46] a) C. R. Corbeil, C. I. Williams, P. Labute, *J. Comput.-Aided Mol. Des.* **2012**, *26*(6), 775–786. b) Z. Wang, Y. Wang, P. Vilekar, S. P. Yang, M. Gupta, M. I. Oh, A. Meek, L. Doyle, L. Villar, A. Brennecke, I. Livanage, M. Reed, C. J. Barden, D. F. Weaver, *PeerJ* **2020**, *7*, e9533. c) M. Gupta, E. F. da Silva, H. F. Svendsen, *J. Phys. Chem. B.* **2013**, *117*(25), 7695–7709. d) S. Livanage, M. Gupta, F. Wu, M. Taylor, M. D. Carter, D. F. Weaver, *Chemotherapy*, **2019**, *64*(1), 22–27.
- [47] L. Zhai, K. L. Lauing, A. L. Chang, M. Dey, J. Qian, Y. Cheng, M. S. Lesniak, D. A. Vainwright, *J. Neurooncol.* **2015**, *123*, 395–403.
- [48] M. Gupta, H. J. Lee, C. J. Barden, D. F. Weaver, *J. Med. Chem.* **2019**, *62*, 9824–9836.
- [49] M. Gupta, T. Bogdanowicz, M. A. Reed, C. J. Barden, D. F. Weaver, *ACS Chem. Neurosci.* **2020**, *11*, 205–224.
- [50] A. Mandal, M. Patel, Y. Sheng, A. K. Mitra, *Curr Drug Targets*, **2016**, *17*, 1773–1798.